

301

20

RM A55H30

NACA RM A55H30

FACILITY FORM 602

<b>N66-19737</b>	
(ACCESSION NUMBER)	(THRU)
<u>20</u>	<u>1</u>
(PAGES)	(CODE)
	<u>01</u>
(NASA CR OR TMX OR AD NUMBER)	(CATEGORY)

GPO PRICE \$ \_\_\_\_\_

CFSTI PRICE(S) \$ \_\_\_\_\_

Hard copy (HC) 1.00

Microfiche (MF) .50

ff 853 July 65

# RESEARCH MEMORANDUM

## SOME INTERFERENCE EFFECTS THAT INFLUENCE VERTICAL-TAIL LOADS AT SUPERSONIC SPEEDS

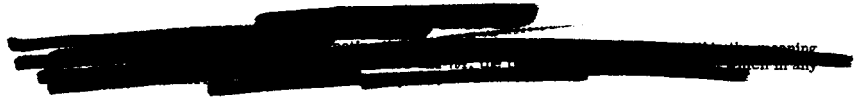
By S. Sherman Edwards

Ames Aeronautical Laboratory  
Moffett Field, Calif.

**DECLASSIFIED  
ATS 480**

**AUTHORITY  
DROBKA TO LEBOW  
MEMO DATED 12/13/65**

Declassified by authority of NASA  
Classification Change Notices No. 43  
Dated \*\*12/29-65



### NATIONAL ADVISORY COMMITTEE FOR AERONAUTICS

WASHINGTON  
February 17, 1956





NATIONAL ADVISORY COMMITTEE FOR AERONAUTICS

RESEARCH MEMORANDUM

AUTHORITY  
 DROBKA TO LEBOW  
 MEMO DATED 12/13/65

SOME INTERFERENCE EFFECTS THAT INFLUENCE VERTICAL-  
 TAIL LOADS AT SUPERSONIC SPEEDS

By S. Sherman Edwards

DECLASSIFIED  
 AT 430

SUMMARY

*19737*

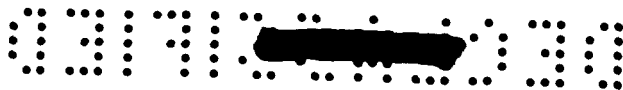
Three types of aerodynamic interference originating from forward components of airplanes are shown to contribute to decreased vertical-tail effectiveness. The vorticity originating from a slender fuselage ahead of the wing resulted in a marked reduction in vertical-tail effectiveness with angle of attack for one model. For another design, location of the vertical tail in a region of reduced dynamic pressure associated with increased supersonic Mach numbers above the wing at angle of attack resulted in decreasing vertical-tail effectiveness with increasing angle of attack. In tests of a third model, pressure waves emanating from externally mounted engine nacelles caused a nonlinear variation of vertical-tail effectiveness with Mach number.

INTRODUCTION

*Quicker*

Flight experiences in which supersonic airplanes were inadvertently subjected to large loads are discussed in references 1 and 2. Deterioration of the directional stability with increasing angle of attack and increasing Mach number was shown to contribute in a large measure to the unexpected violence of the maneuvers experienced. To provide the airplane with sufficient directional stability is the function, primarily, of the vertical-tail component. In recent tests of a number of contemporary airplane models in the Ames 6- by 6-foot supersonic wind tunnel (ref. 3), interference effects of forward lifting components of the models upon the loading on the vertical tail was observed to be an important consideration in determining the effectiveness of this surface. It is the purpose herein to discuss these interference effects in order that their nature and importance might be more fully appreciated, particularly in view of the importance of the directional-stability parameter,  $C_{n\beta}$ , upon the roll-yaw coupling motion discussed in references 1 and 2.





## RESULTS AND DISCUSSION

The variation of the directional stability (or the yawing moment due to sideslip  $C_{n\beta}$ ) with angle of attack at two Mach numbers for a swept-wing airplane is presented in figure 1. The results for this model show a substantial decrease in directional stability with angle of attack and also with Mach number. In fact, a Mach number of 1.9 is well into the speed range in which danger of directional divergence exists. The vertical-tail contribution is the difference between the data for the tail-off and complete configurations. At both Mach numbers, the decrease in the yawing moment due to sideslip with increasing angle of attack is caused by a corresponding decrease in vertical-tail effectiveness. The magnitude of the unstable yawing moment due to sideslip shown for the tail-off configuration illustrates why an efficient vertical tail is needed. For this airplane, the decreased effectiveness of the vertical tail as the angle of attack increases means that to avoid critical tail loads accompanying directional divergence, the size of the surface must be larger than that necessary at small angles of attack.

What are the aerodynamic conditions that combine to rob the vertical tail on this model of its effectiveness as a stabilizing surface? The effect of Mach number is explained adequately by the decreased lift effectiveness of the vertical tail with increasing Mach number. There are, however, three possible explanations of the angle-of-attack effect. Sidewash effects of the wing may be unfavorable. Examination of the increment in  $C_{n\beta}$  between the results for the body-tail and complete configurations indicates, however, that the addition of the wing seems to increase rather than decrease the vertical-tail loading at a given angle of sideslip. The second possibility is that the sweepback of the vertical tail is effectively increased with angle of attack and tends to reduce the effectiveness of the vertical tail because it is known that the lift-curve slope decreases with increasing sweepback. The magnitude of the decrease in vertical-tail effectiveness is much larger than can be traced to this simple explanation. The third possibility is indicated by a study of the body-tail results. Note the marked decrease in the vertical-tail effectiveness with increasing angle of attack. This decrease has been traced to an induced effect of the fuselage in the lifting condition.

With regard to the third possibility, the nature of the induced flow field in the tail region of this model is shown in figure 2 for the fuselage alone at an angle of sideslip of  $5^\circ$  and two angles of attack. These photographs were obtained by means of the vapor-screen technique (see ref. 4) in the Ames 1- by 3-foot supersonic tunnel No. 1. The darkened spots on the vapor screen near the tail of the body are caused by regions of concentrated vorticity associated with the fuselage loading. The spinning action of the vortices forces moisture particles outward from the center of rotation. Innermost areas of the vortices, therefore, are




devoid of moisture particles capable of reflecting light and hence these vortex regions appear as dark spots on the vapor screen. Note that in figure 2 the upper vortex appears to be in the plane of the vertical tail, the position of which is shown in the drawing at the top of figure 1. As the angle of attack was increased from  $8^\circ$  to  $16^\circ$ , this vortex moved upward to approximately the top of the vertical tail.

In figure 3, a similar study of the swept wing in combination with the fuselage is shown. The vantage point from which the vapor screen is observed in this case is located inside the wind tunnel with the model upstream of this point. The light screen is projected from the left in these pictures; consequently, a shadow of the model is cast to the right. In addition to the wing-tip vortices which appear, body vortex regions in the vicinity of the tail are shown. Again, a strong vortex appears in this case somewhat to the right of the plane of the vertical tail. As the angle of attack is increased, this vortex seems to keep approximately the same lateral location with respect to the position of the vertical tail. Forward movement of the vapor screen to the mid-point of the body shows that at this point one of the two body vortices is located under the left wing; the other is above the wing. The marked asymmetry in the body vortex flow, therefore, is readily apparent.

The manner in which these vortices influence the vertical-tail loading is not known quantitatively. Several qualitative statements can be made, however, regarding these vortices and their relationship to the vertical-tail loads: (1) The vertical tail in sideslip is not lifting in a uniform stream and both chordwise and spanwise variations in the loading caused by localized vorticity should be expected. (2) The marked decrease in vertical-tail load with angle of attack of the body-tail combination appears to be related to the fact that, as shown in figure 2, the vortex coming from the right side of the fuselage (looking forward) actually intersects the vertical tail and hence has maximum influence. The point of intersection moved almost to the top of the tail at the maximum angle of attack so that the induced effects would be expected to decrease at larger angles. (3) The vertical movement of this vortex (i.e., the one from the right side of the fuselage) is somewhat restricted by the presence of the wing; it seems, also, to have moved away from the vertical tail (see fig. 3). Consequently, its influence is diminished and the complete configuration has slightly more directional stability throughout the angle-of-attack range.

The effect of an unswept wing upon the results presented in figure 1 is shown in figure 4. This wing had the same span and aspect ratio as the swept wing shown in figure 1. The vertical tail also was changed to an unswept design; however, results for this tail when tested on the original swept-wing model showed an almost identical variation of the vertical-tail effectiveness with angle of attack and with Mach number as that of the original swept tail. The effect of the vortices that were observed in the vapor-screen tests therefore must have been about the

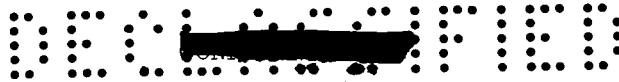


same for the two tails when the fact is considered that the height, area, and chord at the fuselage juncture was kept the same. In figure 4 the data for the unswept-wing model show that the directional stability is maintained and actually increases at moderate angles of attack. The high level as compared with the original airplane is caused by the fact that it was necessary to shift the center of gravity forward slightly to accommodate the more forward position of the unswept-wing center of pressure. For both configurations, the same static margin at a Mach number of 1.5 was maintained. It was estimated that the effect of the straight wing was negligible on the tail-off results shown in figure 1; therefore, it was concluded that the maintenance of directional stability with angle of attack was caused almost entirely by an increase in the vertical-tail effectiveness at high angles of attack.

Vapor-screen photographs of the vortex flow in the tail region of this model are shown in figure 5. From a comparison of these photographs with those for the same model with a swept wing (fig. 3), it appears that the vorticity originating from the right side of the fuselage looking forward is somewhat distributed in character; and the center of gravity of this vorticity passes farther to the right of the vertical-tail position. It is probable also that the forward location of the tip of the unswept wing relative to that of the swept wing increases the sidewash at the vertical tail with a resultant increase in the effectiveness of the vertical tail.

A different type of interference effect upon vertical-tail effectiveness has been observed for configurations similar to that shown in figure 6. The increment in the  $C_{n\beta}$  parameter between the tail-off and complete-model results shows again in this case a decrease in the vertical-tail contribution to the directional stability with increasing angle of attack and increasing Mach number. Although the possibility of vortices associated with the lift of the fuselage forward of the wing is not discounted in this case, it is believed that the major factor contributing to this result is the unusually far forward location of the vertical tail. More specifically, as the angle of attack of this model is increased, the stream following the wing-leading-edge shock wave expands to higher than free-stream Mach numbers across the top of the wing. The vertical tail on this model is in this higher Mach number region. The reduction in the load on the vertical tail caused by the decreased dynamic pressure associated with this expansion reduces the directional stability of the airplane as the angle of attack increases.

Most of the vertical tail of the swept-wing model previously discussed is downstream of the flow region influenced by expanding flow above the wing at Mach numbers lower than 1.9; therefore, a similar type of interference effect was not mentioned as a major contributing factor to the vertical-tail loads. At higher speeds, of course, this effect would become of increasing importance for that configuration.



Another interference effect differing from those previously discussed was observed for the model shown in figure 7. Notice that the increment in  $C_{n\beta}$  between the tail-off results and the curve for the complete model shows a nonlinear variation of the tail contribution to the directional stability with Mach number. This nonlinearity disappeared when the nacelles were removed or when the outboard nacelles were placed on pylons below the wing as shown in dashed outline in the side view of the drawing at the top of figure 7. Expansion waves from the nacelles impinge upon the vertical tail in this arrangement and cause both chordwise and spanwise variations in the loading on the vertical tail and a general decrease in its effectiveness. The nonlinear increase in effectiveness with Mach number is caused by the rearward movement of pressure waves from the nacelles along the vertical tail. This effect causes the directional stability of the complete model to approach the nacelles-off results at a Mach number of 1.9. An important consideration for an airplane having nacelles in this position from the standpoint of vertical-tail design would be the sudden loss of thrust in one of the outboard engines. This condition could result in large differences in the pressure waves impinging on the two sides of the vertical tail and could cause large sideslip angles and large loads on the tail.

#### SUMMARY OF RESULTS

In summary, it is pointed out that a deficiency in directional stability permits the airplane to develop large angles of sideslip and hence large vertical-tail loads. The tail-off yawing moments for each of the models considered were markedly unstable. The vertical tail on the swept-wing model provided adequate directional stability at low angles of attack; however, vorticity associated with the lift of the fuselage decreased the vertical-tail effectiveness as the angle of attack increased. When the wing on this model was changed to an unswept design, the effectiveness of the vertical tail was maintained with increasing angle of attack. This result was believed to be caused primarily by the fact that the unswept wing altered the position of vortices originating from the fuselage ahead of the wing and caused a decrease in the adverse sidewash at the vertical tail.

For the triangular-wing model, a decrease in vertical-tail effectiveness with angle of attack also occurred; this decrease was caused by the location of the tail in a region of reduced dynamic pressure associated with expansion of the flow over the wing. For both airplanes, large vertical tails are necessary to avoid directional divergence and hence excessive tail loads.

An interference effect of a different nature influenced the vertical-tail loads on the model with nacelles located on the wing. In this case,





pressure waves from the nacelles impinged on the vertical tail. At moderate supersonic Mach numbers, these waves influenced the vertical-tail loads in sideslip and caused a nonlinear variation of the directional stability with Mach number.

Ames Aeronautical Laboratory  
National Advisory Committee for Aeronautics  
Moffett Field, Calif., Aug. 30, 1955

#### REFERENCES

1. Zimmerman, Charles H.: Recent Stability and Aerodynamic Problems and Their Implications as to Load Estimation. NACA RM L55E11a, 1955.
2. Weil, Joseph, Gates, Ordway B., Jr., Banner, Richard D., and Kuhl, Albert E.: Flight Experience of Inertia Coupling in Rolling Maneuvers. NACA RM H55E17b, 1955.
3. Smith, Willard G., and Ball, Louis H.: Static Lateral-Directional Stability Characteristics of Five Contemporary Airplane Models From Wind-Tunnel Tests at High Subsonic and Supersonic Speeds. NACA RM A55J03, 1955.
4. Spahr, J. Richard, and Dickey, Robert R.: Wind-Tunnel Investigation of the Vortex Wake and Downwash Field Behind Triangular Wings and Wing-Body Combinations at Supersonic Speeds. NACA RM A53D10, 1953.



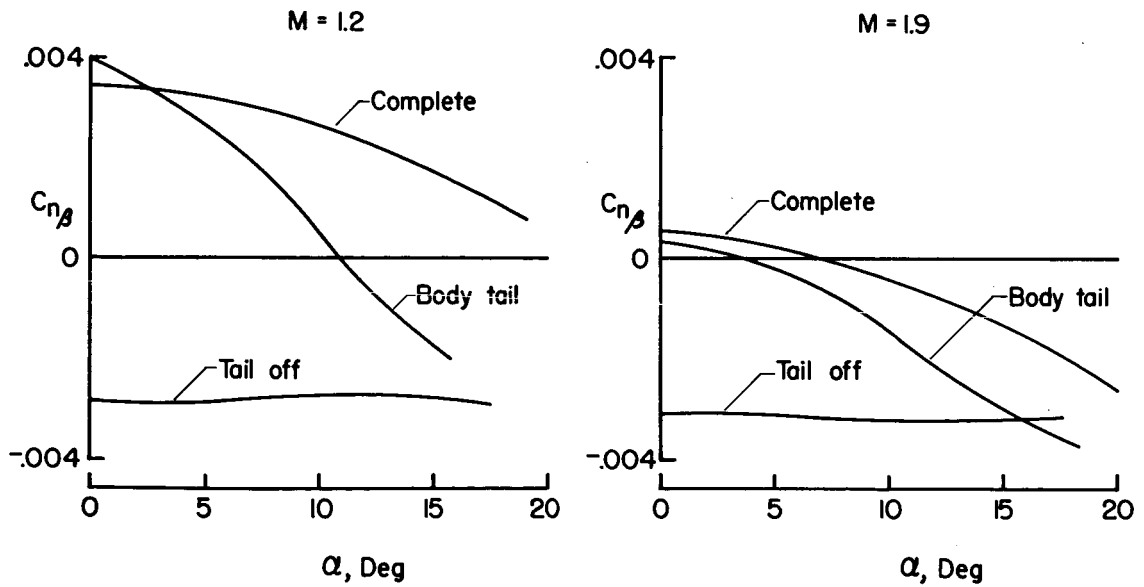
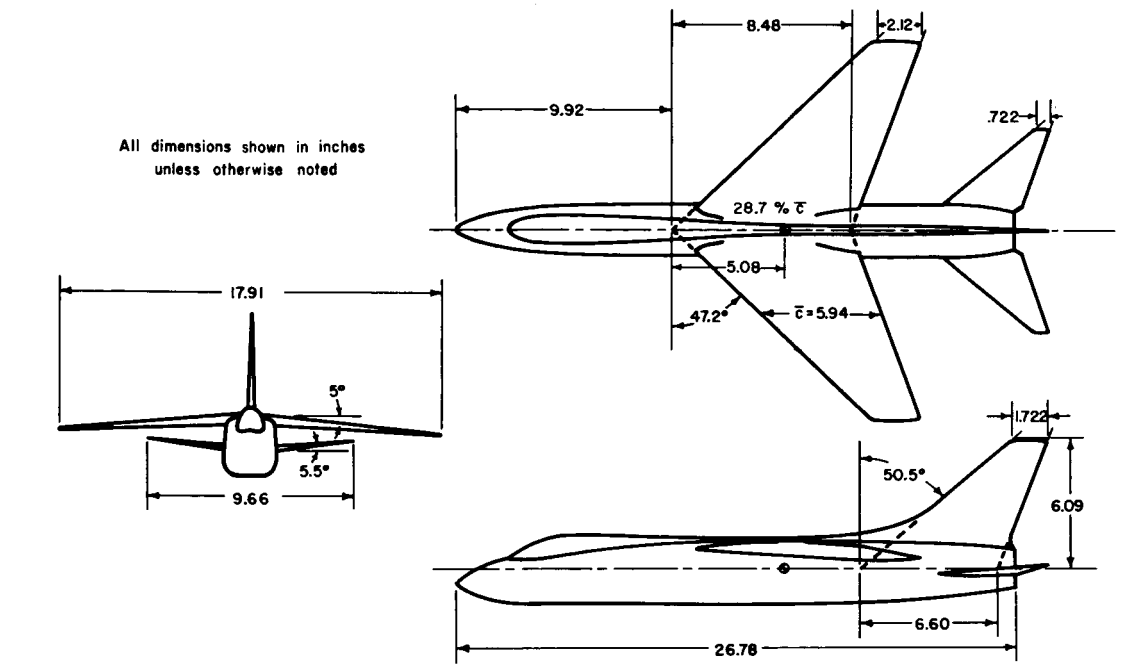
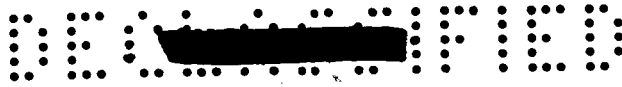


Figure 1. - Vertical-tail effectiveness for a swept-wing airplane.







$\alpha = 8^\circ, \beta = 5^\circ, M = 1.9$



$\alpha = 16^\circ, \beta = 5^\circ, M = 1.9$

Figure 2.- Vapor-screen photographs of fuselage vortices in the tail region.



$\alpha = 6^\circ, \beta = 5^\circ, M = 1.9$



$\alpha = 12^\circ, \beta = 5^\circ, M = 1.9$



$\alpha = 12^\circ, \beta = 5^\circ, M = 1.9$

Vapor screen forward to midpoint of body

Figure 3.- Effect of a swept wing on fuselage vortices viewed directly upstream.



All dimensions shown in inches unless otherwise noted

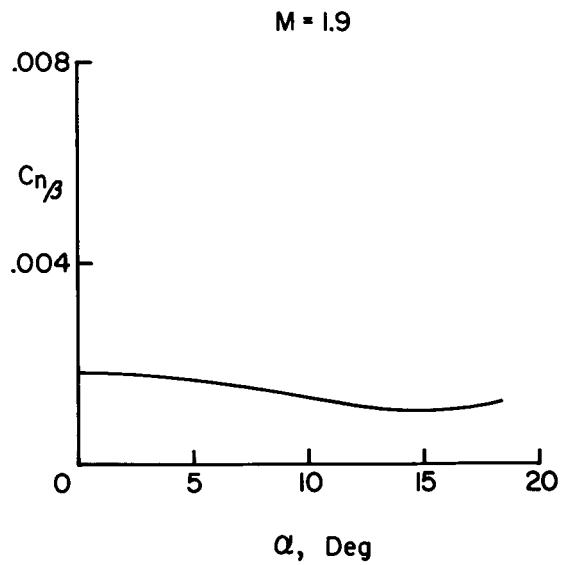
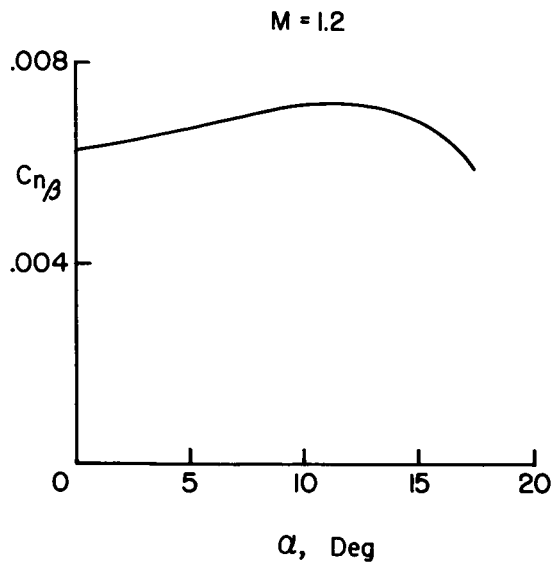
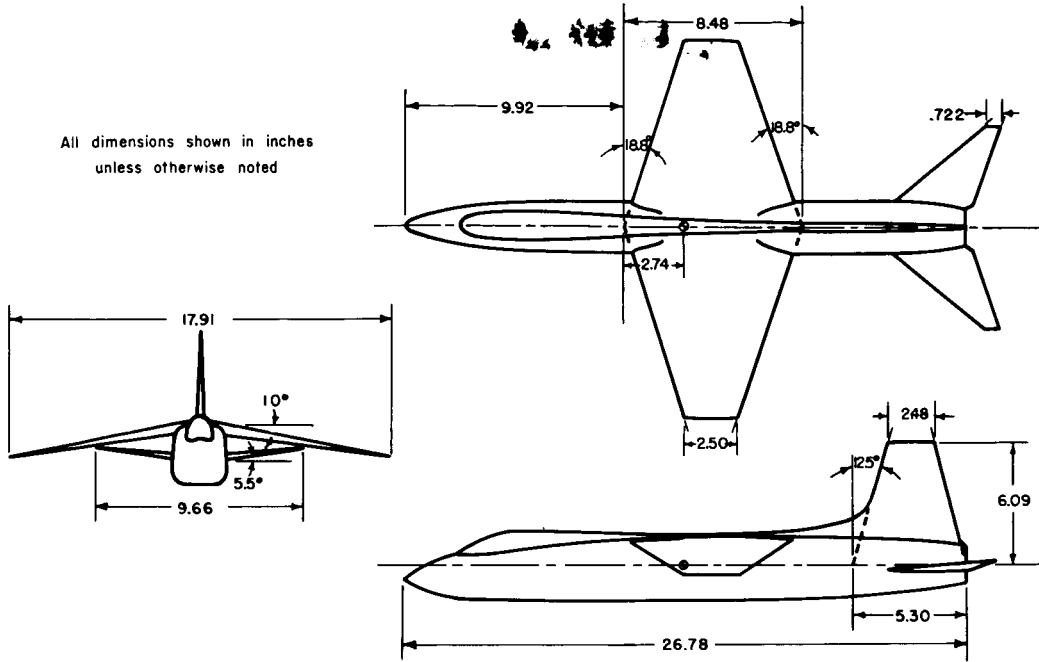
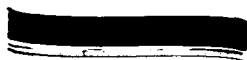
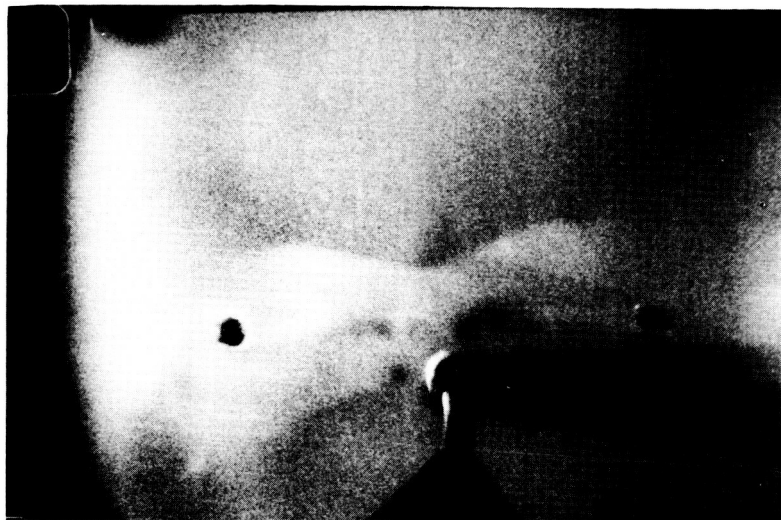
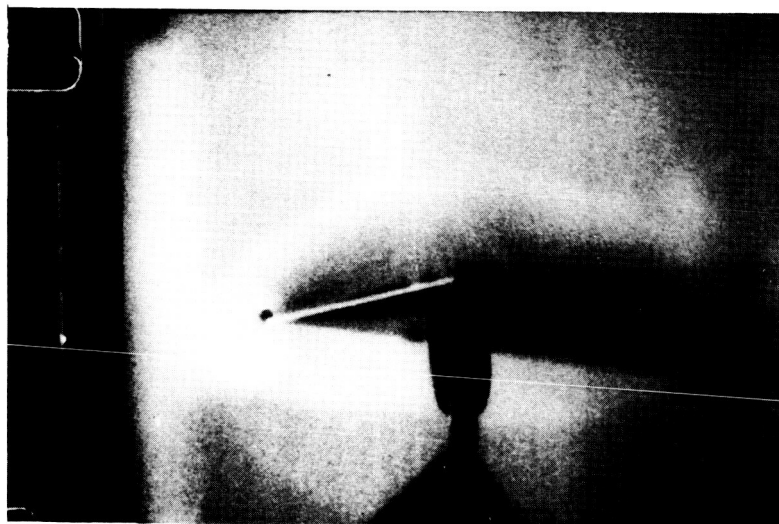


Figure 4.- Effect of an unswept wing.





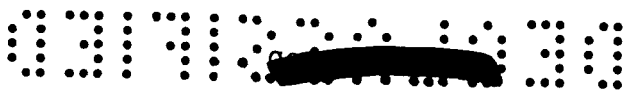
$\alpha = 12^\circ, \beta = 5^\circ, M = 1.9$



$\alpha = 12^\circ, \beta = 5^\circ, M = 1.9$

Vapor screen forward to midpoint of body

Figure 5.- Effect of an unswept wing on fuselage vortices viewed directly upstream.



All dimensions shown in inches unless otherwise noted

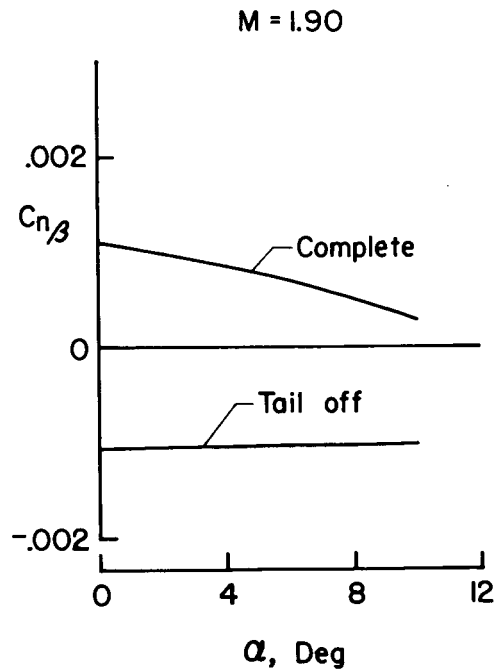
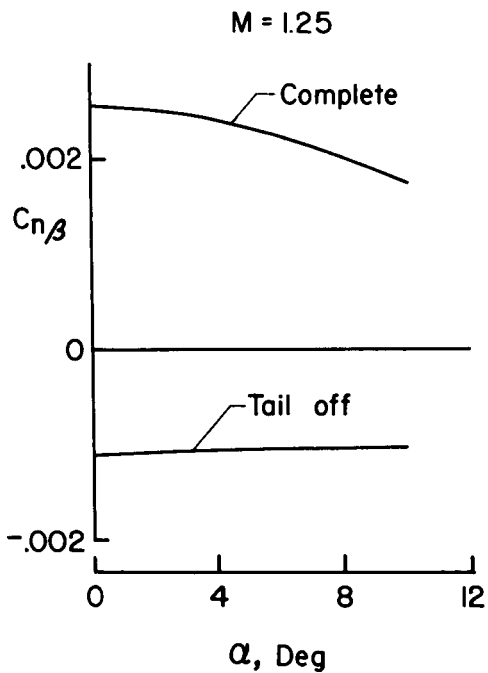
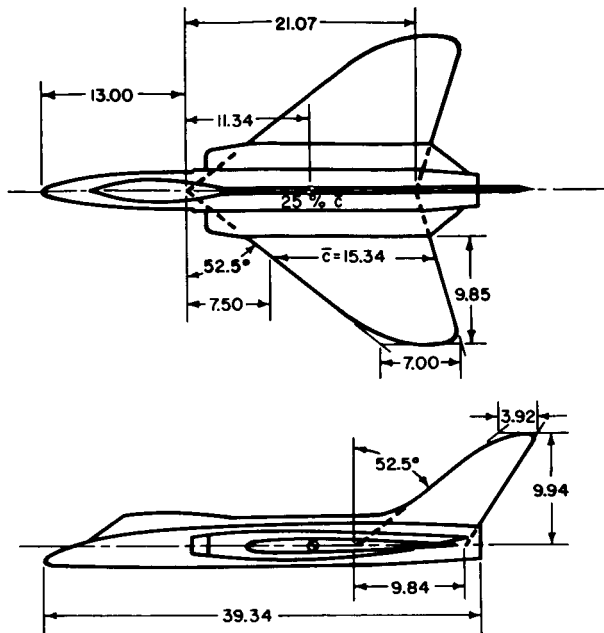
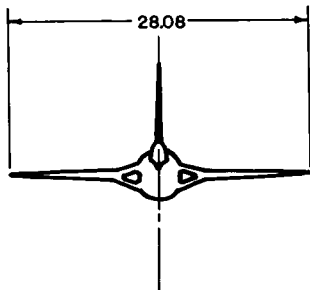


Figure 6.- Vertical-tail effectiveness for a triangular-wing airplane.



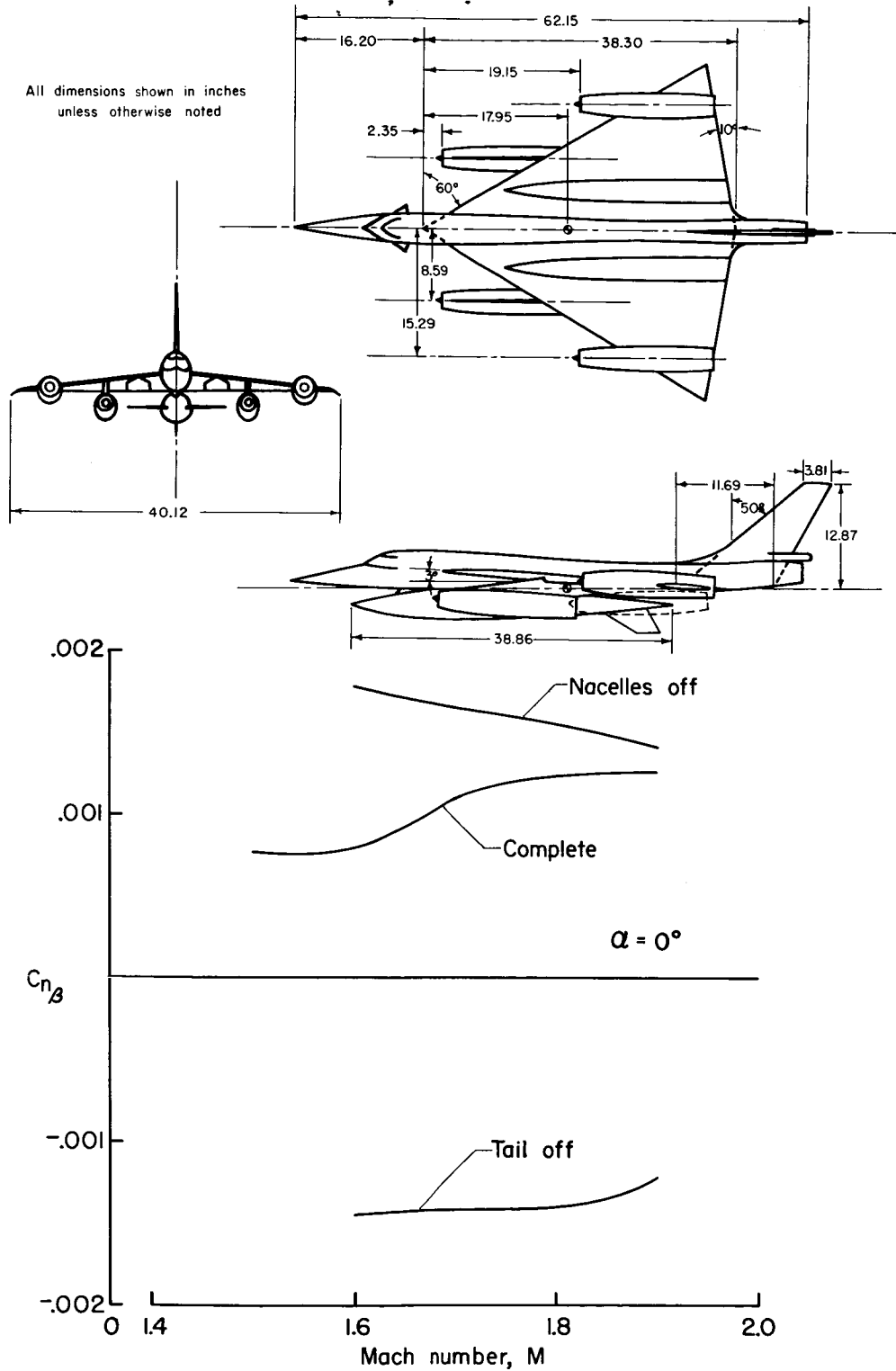


Figure 7.- Effect of nacelles on vertical-tail effectiveness.